System Identification of *Just Walk*: Using Matchable-Observable Linear Parametrizations

Paulo Lopes dos Santos, *Member, IEEE*, Mohammad T. Freigoun, César A. Martín, *Member, IEEE*, Daniel E. Rivera, *Senior Member, IEEE*, Eric B. Hekler, Rodrigo Alvite Romano, *Member, IEEE*, and Teresa P. Azevedo Perdicoúlis

***Abstract*— System identification approaches have been used to design an experiment, generate data, and estimate dynamical system models for *Just Walk*, a behavioral intervention intended to increase physical activity in sedentary adults. The estimated models serve a number of important purposes, such as understanding the factors that influence behavior and as the basis for using control systems as decision algorithms in optimized interventions. A class of identification algorithms known as matchable-observable linear identification has been reformulated and adapted to estimate linear time-invariant models from data obtained from this intervention. The experimental design, estimation algorithms, and validation procedures are described, with the best models estimated from data corresponding to an individual intervention participant. The results provide insights into the individual and the intervention, which can be used to improve the design of future studies.**

***Index Terms*— Behavioral interventions, behavioral sciences, design of experiments, parameter estimation, system identification, systems modeling.**

I. Introduction

THE use of system identification and control theory in the design of optimized interventions for health behaviors, such as healthy eating, increased physical activity (PA), and smoking cessation, has become a problem of significant importance [1]–[3]. Strong evidence exists to show that increasing PA reduces chronic disease risk [4]–[6]. Advances in the science of behavior change reveal that interventions aimed at incorporating PA into one's day-to-day life ought to be personalized and time-varying (i.e., adaptive) [7], [8]. Rising mobile health (mHealth) sensor technologies enabled the use of more cost-effective, convenient, and scalable platforms that are increasingly more practical for the design and delivery of personalized and perpetually adaptive behavioral health interventions tailored for each person's changing needs [9].

In this paper, system identification methods are used to model the dynamics of PA behavior change. Insights are drawn from social cognitive theory (SCT), an important theory for describing health behavior [10]. Martín *et al.* [11], [12] presented a dynamical fluid analogy model of SCT (Fig. 1) to provide a quantitative understanding of behavior change that can ultimately be coupled with model predictive control to design optimal interventions that sustain a healthy level of PA particularly among middle-aged, overweight, and sedentary populations [1], [13]. To accomplish this, the *Just Walk* intervention study, developed by the Designing Health and Control Systems Engineering Labs (both at Arizona State University), was conceived with the aim of reaching a sustained level of daily steps of the participants by the end of the intervention. *Just Walk* represents (to the authors' knowledge) the first behavioral intervention designed from a primarily system identification perspective.

Guided by SCT, in *Just Walk*, changes in daily step goals (an external cue to action, ξ_8 in Fig. 1) and positive reinforcement (given as expected reward points, ξ_9) were specified for each participant using multisine signals as input sequences. In addition, a "granted points" signal (ξ_{10}) was available for each participant based on whether or not the steps performed per day were greater or equal than the specified goal. Furthermore, numerous additional objective and self-reported contextual measurements (e.g., predicted stress, sleep, weather, whether the day is a weekday or weekend) were recorded and represented possible disturbances. Freigoun *et al.* [14] have examined the importance of these signals in personalizing the dynamics for each participant, relying on autoregressive with exogenous inputs (ARX) models.

In this paper, the goal is to develop new identification approaches that can improve the consistency expected from black-box modeling and to examine their usefulness in a novel and nontraditional application setting, namely, a behavioral

Manuscript received March 18, 2018; revised August 8, 2018; accepted November 8, 2018. Date of publication December 24, 2018; date of current version December 27, 2019. Manuscript received in final form November 29, 2018. This work was supported in part by the Fundação para a Ciência e a Tecnologia under Grant SFRH/BSAB/11383572015, in part by the National Science Foundation under Grant IIS-1449751, and in part by the Research Center for Systems and Technology (SYSTEC) of Faculdade de Engenharia da Universidade do Porto. Recommended by Associate Editor A. Medvedev. *(Corresponding author: Paulo Lopes dos Santos.)*

P. Lopes dos Santos is with the Institute for Systems and Computer Engineering, Technology and Science (INESC-TEC), Faculty of Engineering, University of Porto, 4200-464 Porto, Portugal (e-mail: pjsantos@fe.up.pt).

M. T. Freigoun and D. E. Rivera are with the Control Systems Engineering Laboratory, School for Engineering of Matter, Transport, and Energy, Arizona State University, Tempe, AZ 85287 USA (e-mail: m.freigoun@asu.edu; daniel.rivera@asu.edu).

C. A. Martín is with the Facultad de Ingeniería en Electricidad y Computación, Escuela Superior Politécnica del Litoral Polytechnic University, Campus Gustavo Galindo, Guayaquil, Ecuador (e-mail: cmartin@espol.edu.ec).

E. B. Hekler is with the Center for Wireless and Population Health Systems, Department of Family Medicine and Public Health, University of California at San Diego, San Diego, CA 92093 USA (e-mail: ehekler@ucsd.edu).

R. A. Romano is with the Escola de Engenharia do Instituto Mauá de Tecnologia, São Caetano do Sul, SP 09580 Brazil (e-mail: rromano@maua.br).

T. P. Azevedo Perdicoúlis is with the Department of Engineering, Universidade de Trás-os-Montes e Alto Douro, 5001-801 Vila Real, Portugal, and also with the Instituto de Sistemas e Robótica, 3030-194 Coimbra, Portugal (e-mail: tazevedo@utad.pt).

Color versions of one or more of the figures in this article are available online at http://ieeexplore.ieee.org.

Digital Object Identifier 10.1109/TCST.2018.2884833

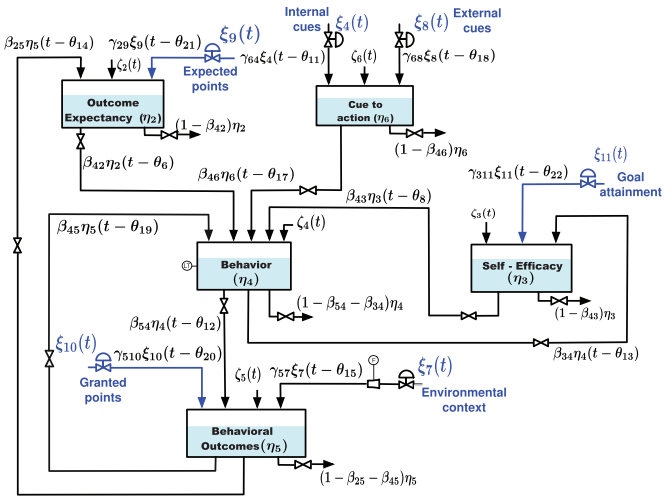

Fig. 1. Fluid analogy describing the dynamics of a simplified model of SCT [10].

Fig. 2. Screenshot of the main window of the *Just Walk* app.

intervention to increase PA. In [15]–[19], a class of algorithms for identifying state-space models for multiple-input-multiple-output systems was proposed. These algorithms rely on parametrizations particularly suited for system identification, restricting the amount of free parameters in the model matrices. Moreover, the parameters are estimated using a linear least squares estimator that, with a proper choice of some design parameters, becomes or can approximate the optimal prediction error (PEM) estimator. This class of algorithms, denoted as matchable-observable linear identification (MOLI), has been reformulated in this paper and adapted to estimate new, alternative linear time-invariant (LTI) models from data gathered in *Just Walk*; these are contrasted to the use of ARX estimation as examined in [14]. Ultimately, the results from black-box estimation set a standard which needs to be met by approaches that can be used to validate the SCT model, such as semiphysical identification [20].

This paper is organized as follows. Section II provides a general description of the *Just Walk* intervention, with emphasis on the input signal design procedure and experimental execution. Section III develops the reformulated MOLI algorithms for *Just Walk* system identification. Section IV highlights the model estimation and validation approach applied in this paper by applying the methods to data from a selected intervention participant. Section V concludes this paper, describing new directions for research resulting from this paper.

II. Description of the *Just Walk* Intervention

Just Walk was developed as an adaptive walking intervention for sedentary, overweight adults. It was designed primarily as a tool to generate individualized computational models for understanding PA behavior via system identification. The intervention system included a front-end Android app, *Just Walk* (Fig. 2), a backend server, and an activity tracker (Fitbit Zip) to objectively measure PA and automatically sync with the smartphone application. Participants were recruited nationally to partake in a walking intervention and receive daily step goals via the *Just Walk* app, and daily announced points were granted if the goals were achieved that day; granted points were converted into Amazon gift cards after a certain threshold was reached. Participants were also required to complete a series of daily morning and evening ecological momentary assessment (EMA [21]) measures (e.g., confidence in achieving goal, predicted business for that day, previous night sleep quality, etc.) for the entire duration of the study.

The study duration was 14 weeks, including an initial two-week baseline period in which no step goals were delivered. Each participant's step goals were then based on their median daily step value as calculated from the 14-day baseline period. The step goals were designed to establish a mechanism for individualizing the definition of an "ambitious, but doable" step range. All PA data were collected from the Fitbit Zip (provided to participants as a part of the study) and stored both locally and in Fitabase (Small Steps Labs, San Diego, CA, USA). Participants were generally healthy, inactive, 40–65 years old, with a body mass index of 25–45 kg/m^2, who currently owned an Android phone capable of connecting to a Fitbit Zip via Bluetooth 4.0 and were willing to engage with the mHealth intervention for the 14-week duration.

It should be noted that the *Just Walk* intervention, besides facilitating an understanding of human behavior change, ultimately achieved a sustained increase in PA in the participant population (with an average increase per participant of 2650 steps per day, from baseline to intervention completion [22]). The ensuing section provides a description of the implemented experimental design.

A. Designing the Input Signal

Input signal design is a crucial step in developing system identification experiments. A block diagram of the *Just Walk* intervention that serves as the basis for input design is depicted in Fig. 3. A reward mechanism is implemented using a point-based system, where rewards are given when a specific number of points has been reached. The behavior is influenced relying on the SCT model from Fig. 1 through the following components.

1) *Daily Goals* (u_8): The desired amount of daily steps performed by individuals (e.g., 10 000) which represents an external cue (ξ_8).

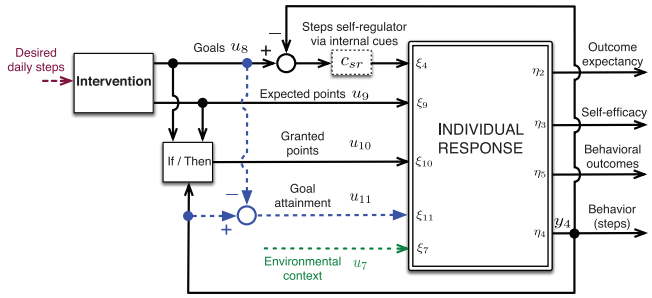

Fig. 3. Block diagram for the *Just Walk* intervention to influence behavior and other constructs. Human (participant) response is represented using the input-output mapping described by the simplified SCT model per Fig. 1.

2) *Expected Points* (u_9): As an outcome expectancy for reinforcement (ξ_9), this number of points is granted if the daily goal is achieved.
3) *Granted Points* (u_{10}): As a reinforcement (ξ_{10}) through an "If/Then" block that delivers the announced expected points ($u_{10} = u_9$) only if the daily goal is achieved ($y_4 \geq u_8$).

In this setting, there are only two exogenous signals that are considered as inputs to the system: *Daily goals* (u_8) and *Expected points* (u_9).

Input signals for the *Just Walk* experiment are designed with the goal of exciting different frequency grids for each signal; orthogonal ("zippered") multisine signals are used for this purpose [23]. Multisine inputs are deterministic, periodic signals whose frequency spectrum is specified by the designer. Each input u_n ($n = 8, 9$) is described as a sum of sinusoids according to

$$u_n(k) = \lambda_n \sum_{j=1}^{N_s/2} \sqrt{2\alpha_{[n,j]}} \cos(\omega_j k T_s + \phi_{[n,j]})$$
$$\omega_j = \frac{2\pi j}{N_s T_s}, \quad k = 1, \ldots, N_s \tag{1}$$

where λ_n is the scaling factor, N_s is the signal period, and T_s is the sampling time. For each harmonic: $\alpha_{[n,j]}$ is a Fourier coefficient used to define the specific power of the harmonic, ω_j is the frequency, and $\phi_{[n,j]}$ is the phase. $\alpha_{[n,j]}$ are chosen to obtain input signals that are excited orthogonally in frequency; each input signal channel has power at unique points in the frequency grid. For the case of two signals, these are orthogonal if a nonzero Fourier coefficient in a specific frequency of one signal implies a zero-valued Fourier coefficient at the same frequency for the other signal. The corresponding arrangement (shown for $n_u = 2$ inputs in Fig. 4) is referred to as a "zippered" spectrum design [23]. If n_s is the total amount of independently excited sinusoids per channel, then the "zippered" spectrum for each signal u_n can be defined by specifying

$$\alpha_{[n,j]} = \begin{cases} 1, & \text{if } j = n_u(i-1) + (n-7) \\ & \text{for } i = 1, 2, \ldots n_s \\ 0, & \text{otherwise} \end{cases}. \tag{2}$$

The signal period N_s must be carefully chosen, since it needs to be long enough to contain the dominant dynamic

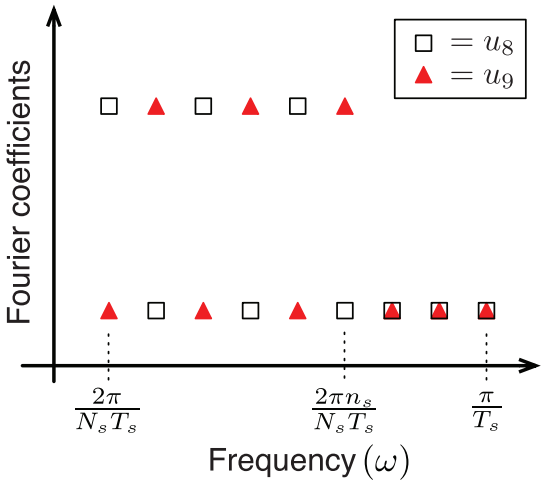

Fig. 4. Conceptual representation for a $n_u = 2$ channel "zippered" spectrum design with $n_s = 6$ independently excited sinusoids, yielding $n_h = 6$ harmonics and selecting $N_s = 18$.

information of the system, and at the same time short enough to reduce the extent of experimental testing. The required number of sinusoids per channel n_s can be estimated relying on available *a priori* information about the model order by

$$\text{Model order} \leq n_s. \tag{3}$$

The range of usable frequencies is given by (1) as

$$\frac{2\pi}{N_s T_s} \leq \omega \leq \frac{2\pi n_s}{N_s T_s} < \frac{\pi}{T_s} \tag{4}$$

from where a bound for N_s can be derived as

$$N_s > 2n_s. \tag{5}$$

Therefore, the total duration of the experiment N (in terms of sampling instants) is

$$N = N_s M > 2n_s M. \tag{6}$$

For the *Just Walk* intervention, the sampling time of the process is 1 day; hence, the number of frequencies and samples per period cannot be large to keep the cycle length reasonable. With this in mind, considering at least three frequency points of analysis for each input, and assuming that no other prior information about the model order is available, $n_s = 6$ was chosen. Relying on (5) $N_s = 14$ days could be our first selection for the signal period; however, because having a biweekly cycle might cause some type of familiarization of the participant with the same goal occurring on identical days (i.e., every first Monday a goal of 8000 steps, every second Tuesday a goal of 9000 steps); correspondingly a period of $N_s = 16$ days was selected.

The input signals were repeated for M cycles such that the total duration of the experiment is $N_s M$ days. Phases ϕ were selected to minimize the crest factor of the signal using the approach of Guillaume *et al.* [24].

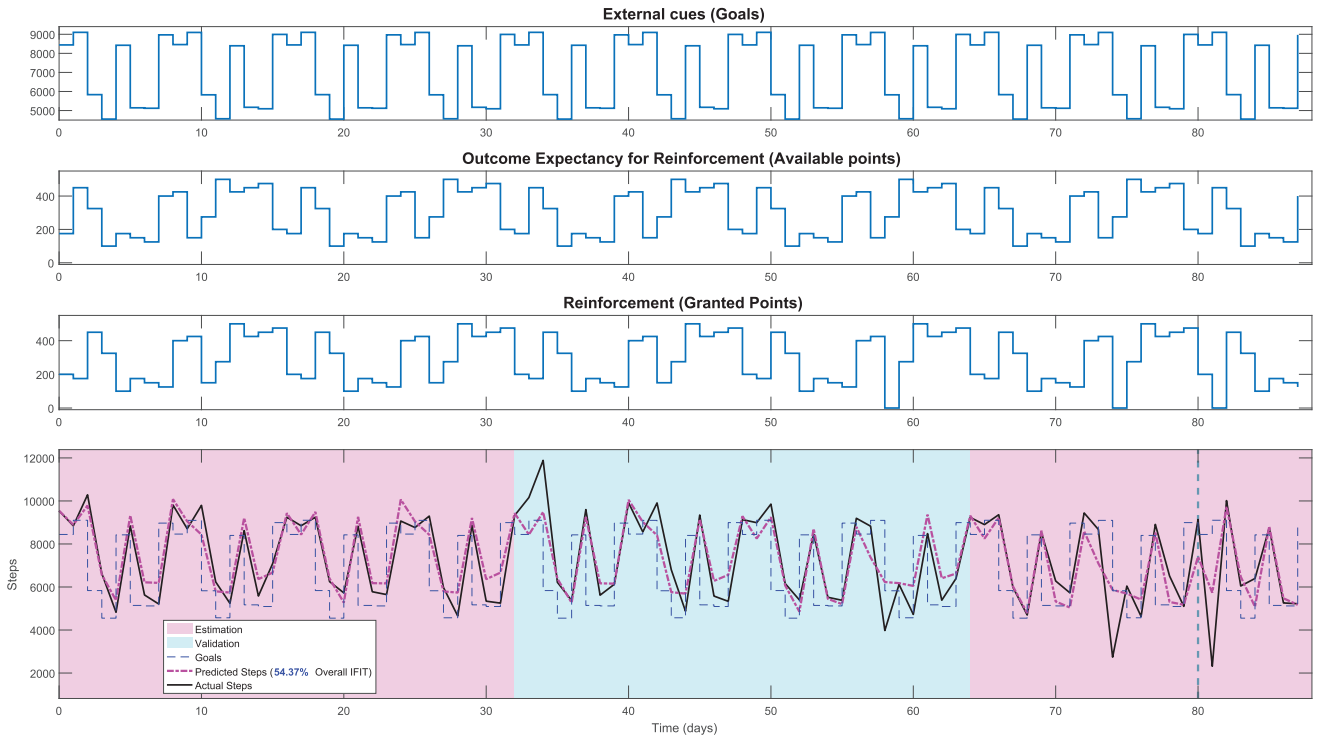

Fig. 5. Time series plot showing the three input sequences (manipulated inputs), and estimation and validation cycles (first, second, and fifth for estimation; third and fourth for validation) for an individual *Just Walk* participant, model estimated with the PEM-MOLI algorithm initialized with Polytope-MOLIZoft.

B. Intervention Implementation

In this paper, an app (Fig. 2) was developed to upload and download the relevant participant data (objective and self-reported measurements). As noted previously, study duration was 14 weeks, including an initial two-week baseline period in which no step goals were delivered. Amplitudes of the designed input signals in (1) were selected to establish a mechanism for individualizing the definition of an "ambitious, but doable" step range [25]. Moreover, participants received daily step goals via the *JustWalk* app, and daily announced points were granted if the goals were achieved that day; granted points were converted into gift cards after a certain threshold of total points was reached. Fig. 5 displays the designed "zippered," multisine *Goals*, and *Expected Points* input signals as well as the recorded *Granted Points* as a result of the measured output in walked steps/day (plotted in Fig. 5 in black solid line). Furthermore, details regarding available measurements of *Just Walk* are presented in [14], [22], and [25].

III. Multiple-Input-Single-Output MOLI Algorithms

Consider, the following state-space realization of an LTI multiple-input-single-output (MISO) system with a strictly proper transfer function

$$x(k+1) = Ax(k) + Bu(k) + Ke(k) \tag{7}$$

$$y(k) = Cx(k) + e(k) \tag{8}$$

where $e(k)$ is the zero-mean white-noise, $x(k) \in \mathbb{R}^{n_x}$, $u(k) = [u_1(k) \quad \cdots \quad u_{n_u}(k)]^T \in \mathbb{R}^{n_u}$, $y(k) \in \mathbb{R}$, $A \in \mathbb{R}^{n_x \times n_x}$

$$B = \begin{bmatrix} B_1 & B_2 & \cdots & B_{n_u} \end{bmatrix} \in \mathbb{R}^{n_x \times n_u} \tag{9}$$

$C \in \mathbb{R}^{1 \times n_x}$, and $K \in \mathbb{R}^{n_x}$. Decompose the state matrix A as

$$A = A_0 + LC \tag{10}$$

where $L \in \mathbb{R}^{n_x}$. The state equation may be rewritten as

$$x(k+1) = (A_0 + LC)x(k) + Bu(k) + Ke(k). \tag{11}$$

Replacing, $Cx(k)$ by the value given in the output equation, it becomes

$$x(k+1) = A_0 x(k) + Ly(k) + Bu(k) + (K - L)e(k). \tag{12}$$

Here, because $y(k)$ is known (measured) it may be seen as an additional input of the state-space equation. As a result, $x(k)$ can be calculated from

$$x(k) = A_0^{k-1}x(1) + (qI - A_0)^{-1}[Ly(k) + Bu(k) + (K - L)e(k)] \tag{13}$$

where q is the shift forward operator. The output equation is now given as

$$\begin{aligned} y(k) &= CA_0^{k-1}x(1) \\ &\quad + C(qI - A_0)^{-1}(Ly(k) + Bu(k)) + e(k) \\ &= CA_0^{k-1}x(1) + C(qI - A_0)^{-1}Ly(k) \\ &\quad + \sum_{i=1}^{n_u} C(qI - A_0)^{-1}B_i u_i(k) \\ &\quad + [C(qI - A_0)^{-1}(K - L) + 1]e(k). \end{aligned} \tag{14}$$

Since $y(k)$ and $u_i(k)$ are scalars, this equation may be rewritten as

$$y(k) = CA_0^{k-1}x(1) + y_f^T(k)L + \sum_{i=1}^{n_u} u_{if}^T(k)B_i + e_y(k) \quad (15)$$

where

$$y_f(k) = \left(qI_{n_x} - A_0^T\right)^{-1}C^T y(k) \in \mathbb{R}^{n_x \times 1} \quad (16)$$

$$u_{if}(k) = \left(qI_{n_x} - A_0^T\right)^{-1}C^T u_i(k) \in \mathbb{R}^{n_x \times 1}, \quad i = 1, \ldots, n_u \quad (17)$$

$$e_y(k) = \left[C\left(qI_{n_x} - A_0^T\right)^{-1}(K - L) + 1\right]e(k). \quad (18)$$

That is, $y_f(k)$ and $u_{if}(k)$, for $i = 1, \ldots, n_u$ are the outputs of the system $(A_0^T, C^T, I_{n_x}, 0_{n_x})$ excited by $y(k)$ and $u_i(k)$, for $i = 1, \ldots, n_u$, respectively, and $e_y(k)$ is the noise term. If C and A_0 are known, B and L can be calculated by a linear least squares estimator and A can be derived from A_0 and L. Furthermore, if the previously set pair (C, A_0) is observable, the state-space model $(A_0 + LC, B, C, 0_{1\times n_u})$ can be a realization of any MISO transfer function for adequate values of L and B.

Putting together CA_0^{k-1} and the regressors $y_f^T(k)$ and $u_{if}^T(k)$ in

$$\varphi(k) = \begin{bmatrix} CA_0^{k-1} & y_f^T(k) & u_{1f}^T(k) & \cdots & u_{n_u f}^T(k) \end{bmatrix} \quad (19)$$

and $x(1)$, L, and B_i in

$$\begin{aligned} \theta &= \begin{bmatrix} x^T(1) & L^T & B_1^T & \cdots & B_{n_u}^T \end{bmatrix}^T \\ &= \begin{bmatrix} x^T(1) & L^T & \text{vec}\,(B)^T \end{bmatrix}^T. \end{aligned} \quad (20)$$

Equation (15) may be rewritten in the following condensed form:

$$y(k) = \varphi(k)\theta + e_y(k). \quad (21)$$

As a result, a set of N noisy observations may be described by

$$Y = \Phi\theta + \mathcal{E} \quad (22)$$

where

$$Y = \begin{bmatrix} y(1) & \cdots & y(N) \end{bmatrix}^T \quad (23)$$

$$\Phi = \begin{bmatrix} \varphi(1)^T & \cdots & \varphi^T(N) \end{bmatrix}^T \quad (24)$$

$$\mathcal{E} = \begin{bmatrix} e_y(1) & \cdots & e_y(N) \end{bmatrix}^T. \quad (25)$$

If $\Phi^T\Phi$ is nonsingular, the least squares estimator which minimizes the cost function

$$J = \frac{1}{2}(Y - \Phi\theta)^T(Y - \Phi\theta) \quad (26)$$

is given by the well-known formula

$$\hat{\theta} = (\Phi^T\Phi)^{-1}\Phi^T Y. \quad (27)$$

Since the regressor $\varphi(k)$ contains the noisy signal $y_f(k)$, $\hat{\theta}$ may not be a consistent estimator. However, once $y_f(k)$ is derived by filtering $y(k)$ through $(qI - A_0^T)^{-1}C^T$, an appropriate choice of A_0 may significantly reduce the bias and the variance of $\hat{\theta}$, making it a good estimator. Hence, A_0 is a critical parameter. Bad choices of A_0 will lead to inaccurate models while good choices lead to excellent models. From (18), it can be seen that if $L = K$, the PEM $e_y(k)$ becomes white noise. As a result, $A_0 = A + KC$ is the optimal value of A_0 and the minimal of J is a PEM estimator. In what follows, some approaches to determine A_0 are proposed.

A. ARX MOLI

The estimated state-space realization is in the form

$$A = \begin{bmatrix} 0 & 0 & \cdots & 0 & -a_{n_x} \\ 1 & 0 & \cdots & 0 & -a_{n_x-1} \\ \vdots & \vdots & \ddots & \vdots & \vdots \\ 0 & 0 & \cdots & 1 & -a_1 \end{bmatrix} \quad B = \begin{bmatrix} b_{n_x} \\ b_{n_x-1} \\ \vdots \\ b_1 \end{bmatrix}$$
$$C = \begin{bmatrix} 0 & 0 & \cdots & 0 & 1 \end{bmatrix} \quad (28)$$

which is an observable canonical realization of the transfer function

$$H(q) = \frac{b_1 q^{n_x-1} + \cdots + b_{n_x-2}q^2 + b_{n_x-1}q + b_{n_x}}{q^{n_x} + a_1 q^{n_x-1} + \cdots + a_{n_x-2}q^2 + a_{n_x-1}q + a_{n_x}} \quad (29)$$

with $b_i \in \mathbb{R}^{1\times n_u}$, $i = 1, \ldots, n$. If, in (27), A_0 is set to

$$A_0 = \begin{bmatrix} 0 & 0 & \cdots & 0 & 0 \\ 1 & 0 & \cdots & 0 & 0 \\ \vdots & \vdots & \ddots & \vdots & \vdots \\ 0 & 0 & \cdots & 1 & 0 \end{bmatrix} \quad (30)$$

it can be shown that $\hat{\theta}$ is the ARX least squares estimator [15].

B. MOLIZoft Algorithms

A derivative-free optimization method called barycentre was proposed in [16] to find an A_0 matrix leading to suboptimal estimates. The estimated state-space realization is also in the observable canonical form shown in (28). Hence, A_0 is likewise in the companion form and the optimization problem reduces to the determination of the coefficients of its characteristic polynomial. A blind choice of these coefficients can easily lead to an unstable filter $(qI - A_0^T)^{-1}C^T$. To avoid this, the coefficients are calculated from the eigenvalues of A_0. A matrix A_{0_i} with eigenvalues $\Lambda_i = \begin{bmatrix} \lambda_{i_1} & \cdots & \lambda_{i_{n_x}} \end{bmatrix}^T \in \mathbb{R}^{n_x}$, is denoted as the *curiosity* i. If there are n_c curiosities, then A_0 is the barycentre of these curiosities, given as

$$A_0 = \frac{\sum_{i=1}^{n_c} A_{0_i} \exp(-\mu J(A_{0_i}, \mathcal{D}))}{\sum_{i=1}^{n_c} \exp(-\mu J(A_{0_i}, \mathcal{D}))} \quad (31)$$

where $J(A_{0_i}, \mathcal{D})$ is a functional which quantifies the performance of A_{0_i} given a data set $\mathcal{D} = \{u(1), y(1), u(2), y(2), \ldots, u(N), y(N)\}$. Therefore, A_0 is the barycentre of the curiosity points A_{0_i}, $i = 1, \ldots, n_c$, weighted by the term $\exp\left(\mu J(A_{0_i}, \mathcal{D})\right)$. The constant $\mu \in \mathbb{R}_+$ is used to adjust the weighting terms—the higher μ, the more A_0 tends to an element that provides the lowest J (best performance). The rationale behind this method is that curiosity points with better performance have more weight than those with *worse* results. Notice that considerable freedom is retained in the choice of J, as its derivatives are not required. Instead, only the numerical values of the functional have to be computed for each A_{0_i}. For this reason, the barycentre can be seen as a direct optimization method.

The identification algorithms using the MOLI parametrization and the barycentre to optimize A_0 were named as MOLIZoft by Romano and Pait [16] (MOLI from the parameterization and Zoft from zero-order filter tuning because free derivative optimization algorithms are known as zero-order methods and the optimization of A_0 is similar to a filter tuning). In order to approximate the PEM estimator, the performance indexes are the values of the cost function J defined in (26). In [16], the curiosities are parametrized using a pair of dominant complex eigenvalues. Since this procedure can limit the possible range of curiosities, two different ways of generating curiosities were considered here.

1) *Polytopic Barycentre:* The eigenvalues of the curiosities are the real and complex vertexes of a polytope defined by a pair of lower and upper limits, M_n and M_x, respectively, with $-1 < M_n < 1$ and $M_n < M_x < 1$. These vertices are the columns of the following matrix:

$$\begin{array}{ccccccccc} M_n & M_x & M_x & \vdots & M_x & \lambda_c & \vdots & \lambda_c & \vdots & \lambda_c \\ M_n & M_n & M_x & \vdots & M_x & \lambda_c^* & \vdots & \lambda_c^* & \vdots & \lambda_c^* \\ M_n & M_n & M_n & \vdots & M_x & M_n & \vdots & M_x & \vdots & \lambda_c \\ \vdots & \vdots & \vdots & \vdots & \vdots & \vdots & \vdots & \vdots & \vdots & \vdots \\ M_n & M_n & M_n & \vdots & M_x & M_n & \vdots & M_x & \vdots & \lambda_c^* \end{array}$$

when n_x is even and

$$\begin{array}{ccccccccc} M_n & M_x & M_x & \vdots & M_x & \lambda_c & \vdots & \lambda_c & \vdots & \lambda_c \\ M_n & M_n & M_x & \vdots & M_x & \lambda_c^* & \vdots & \lambda_c^* & \vdots & \lambda_c^* \\ M_n & M_n & M_n & \vdots & M_x & M_n & \vdots & M_x & \vdots & \lambda_c \\ \vdots & \vdots & \vdots & \vdots & \vdots & \vdots & \vdots & \vdots & \vdots & \vdots \\ M_n & M_n & M_n & \vdots & M_x & M_n & \vdots & M_x & \vdots & M_x \end{array}$$

when n_x is odd, where

$$\lambda_c = (M_n + M_x)/2 - j\sqrt{M_x^2 - (M_n + M_x)^2/4}.$$

The underlying idea is to generate a set of curiosities with *stable* eigenvalues populating a certain region of the complex plane.

2) *Random Barycentre:* 2^{n_x} curiosities are generated corresponding to characteristic polynomials with random real eigenvalues uniformly distributed in the interval (M_n, M_x), where $-1 < M_n < 1$ and $M_n < M_x < 1$.

C. Output MOLI

In this section, the optimal choice of A_0 is derived when $K = 0$. Under this condition, the PEM is

$$e_y(k) = [-C(qI - A_0)^{-1}L + 1]e(k). \tag{32}$$

Therefore, when $L = 0$, $e_y(k)$ becomes white noise and (27) is an optimal estimator. Hence, from (10), the optimal A_0 is $A_0 = A$. Since A is not previously known, it is impossible to find the optimal estimator without any previous knowledge. It can be found using a fixed point iteration algorithm that, in each iteration, uses as A_0 the A matrix estimated in the previous iteration.

D. PEM-MOLI

The cost function J defined in (26) is a function of the parameters A_0, L, and B, which can be rewritten

$$J(A_0, L, B) = \frac{1}{2}\sum_{k=1}^{N} e_y^2(k, A_0, L, B). \tag{33}$$

As the PEM is a nonlinear function of only A_0 (via $y_f(k)$ and $u_{i_f}(k)$), a separable least squares setting is a natural approach to minimize J. In this manner, the dimension of the optimization parameter space is reduced to the number of parameters of A_0. Therefore, A_0 should be in a companion form so this number is as small as possible. Due to the freedom in choosing C, a canonical observable form is the most suitable state-space realization for the estimated model, because it yields a predictor state-matrix A_0 in the companion form

$$\begin{aligned} A_0 &= \begin{bmatrix} 0 & 0 & \cdots & 0 & -(a_{n_x} + k_{n_x}) \\ 1 & 0 & \cdots & 0 & -(a_{n_x-1} + k_{n_x-1}) \\ \vdots & \vdots & \ddots & \vdots & \vdots \\ 0 & 0 & \cdots & 1 & -(a_1 + k_1) \end{bmatrix} \\ &= \begin{bmatrix} 0 & 0 & \cdots & 0 & -\alpha_{n_x} \\ 1 & 0 & \cdots & 0 & -\alpha_{n_x-1} \\ \vdots & \vdots & \ddots & \vdots & \vdots \\ 0 & 0 & \cdots & 1 & -\alpha_1 \end{bmatrix} \end{aligned} \tag{34}$$

with k_i being the $(n_x - i + 1)^{\text{th}}$ entry of K. As a result, the identification problem can be formulated as follows: given a set of input–output data $(u(k), y(k))$, $k = 1, \ldots, N$, estimate the state-space canonical observable form model by minimizing (33). Defining

$$Y = \begin{bmatrix} y(1) & y(2) & \cdots & y(N) \end{bmatrix}^T \tag{35}$$

$$\Phi(\alpha) = \begin{bmatrix} \Gamma_N & Y_f & U_f \end{bmatrix} \tag{36}$$

with

$$\Gamma_N = \begin{bmatrix} C^T & (CA)^T & \cdots & \left(CA^{N-1}\right)^T \end{bmatrix}^T \tag{37}$$

$$Y_f = \begin{bmatrix} y_f(1) & y_f(2) & \cdots & y_f(N) \end{bmatrix}^T \tag{38}$$

$$U_f = \begin{bmatrix} u_{1f}^T(1) & u_{2f}^T(1) & \cdots & u_{n_u f}^T(1) \\ u_{1f}^T(2) & u_{2f}^T(2) & \cdots & u_{n_u f}^T(2) \\ \vdots & \vdots & \vdots & \vdots \\ u_{1f}^T(N) & u_{2f}^T(N) & \cdots & u_{n_u f}^T(N) \end{bmatrix} \in \mathbb{R}^{N \times n_x n_u} \tag{39}$$

and

$$\theta = \begin{bmatrix} x(1)^T & \text{vec}(L)^T & \text{vec}(B)^T \end{bmatrix}^T \tag{40}$$

$$\alpha = \begin{bmatrix} \alpha_1 & \alpha_2 & \cdots & \alpha_{n_x} \end{bmatrix}^T \tag{41}$$

the cost function (33) can be rewritten as

$$J(\alpha, \theta) = \frac{1}{2}\left[Y - \Phi(\alpha)\theta\right]^T \left[Y - \Phi(\alpha)\theta\right]. \tag{42}$$

Given that the error is a linear function of θ, for a fixed α, θ is the least squares estimator

$$\theta(\alpha) = \Phi^{\dagger}(\alpha)Y \tag{43}$$

where † denotes the pseudoinverse. However, since Φ is a function of α, θ is also a function of α. Using (40) in (33), the cost function is also given as

$$J(\alpha) = \frac{1}{2} Y^T \Pi_\Phi^\perp(\alpha) Y \tag{44}$$

where $\Pi_\Phi^\perp(\alpha)$ is the operator projection into the column space of $\Phi(\alpha)$ orthogonal complement, given as

$$\Pi_\Phi^\perp(\alpha) = I_N - \Pi_\Phi(\alpha) \tag{45}$$

with $\Pi_\Phi(\alpha)$ being the projection operator

$$\Pi_\Phi(\alpha) = \Phi\Phi^\dagger. \tag{46}$$

In the sequel, for the sake of simplicity, α will be dropped from θ, Φ, Π_Φ, and $\Pi_\Phi^\perp$. Using a Gauss–Newton method to minimize V, α is updated iteratively

$$\alpha^{(i+1)} = \alpha^{(i)} - \left(\frac{d\left(\Pi_\Phi^\perp Y\right)}{d\alpha^T} \right)^\dagger \Pi_\Phi^\perp Y. \tag{47}$$

In [26], it is shown that

$$\frac{d\left(\Pi_\Phi^\perp Y\right)}{d\alpha^T} \approx -\Pi_\Phi^\perp \frac{d\Phi}{d\alpha^T} (I_{n_x} \otimes \theta) \tag{48}$$

where $\otimes$ stands for the Kronecker product, θ is given by (43) and

$$\frac{dM}{d\beta^T} = \begin{bmatrix} \frac{dM}{d\beta_1} & \frac{dM}{d\beta_2} & \cdots & \frac{dM}{d\beta_n} \end{bmatrix} \tag{49}$$

for any matrix M and vector $\beta = \begin{bmatrix} \beta_1 & \beta_2 & \cdots & \beta_n \end{bmatrix}^T \in \mathbb{R}^n$. Therefore, α is updated by

$$\alpha^{(i+1)} = \alpha^{(i)} + \left(\Pi_\Phi^\perp \frac{d\Phi}{d\alpha^T} (I_{n_x} \otimes \theta) \right)^\dagger \Pi_\Phi^\perp Y \Big|_{\alpha=\alpha^{(i)}}. \tag{50}$$

As $\alpha \in \mathbb{R}^{n_x}$, then, from (49), $(d\Phi/d\alpha^T)$ has n_x column blocks being the jth block given as

$$\frac{d\Phi}{d\alpha_j} = \begin{bmatrix} \frac{\partial \Gamma_N}{\partial \alpha_j} & \frac{\partial Y_f}{\partial \alpha_j} & \frac{\partial U_{f_1}}{\partial \alpha_j} & \cdots & \frac{\partial U_{f_{n_u}}}{\partial \alpha_j} \end{bmatrix} \tag{51}$$

where $(\partial \Gamma_N / \partial \alpha_j)$ is a matrix whose rows are given as

$$\left(\frac{\partial \Gamma_N}{\partial \alpha_j} \right)_i = \begin{cases} 0_{1\times n_x}, & i = 0 \\ \dfrac{\partial \left(C A_0^i \right)}{\partial \alpha_j}, & i = 1, \ldots, N-1 \end{cases} \tag{52}$$

with $(\partial A_0 / \partial \alpha_i)$ being a matrix with $(\partial A_0 / \partial \alpha_i)_{n_x, n_x+1-i} = -1$ and all other entries equal to zero. It can be shown that the k^{th} rows of $(\partial Y_f / \partial \alpha_j)$ and $(\partial U_{f_i} / \partial \alpha_j)$, $i = 1, \ldots, n_u$, are the transposed outputs of the system

$$\chi(k+1) = A_0^T \chi(k) - \begin{bmatrix} 0 & \cdots & 1 \end{bmatrix}^T v(k) \tag{53}$$

$$\psi(k) = \chi(k) \tag{54}$$

with inputs $v(k) = y_{f_{n_x+1-j}}(k)$ and $v(k) = u_{if_{n_x+1-j}}(k)$, $i = 1, \ldots, n_u$, i.e., the $(n_x + 1 - j)$th entries of $y_f(k)$ and $u_{if}(k)$.

E. Relation Between the PEM-MOLI and the ARMAX Prediction Error Estimators

The input–output model equivalent to the state-space realization in (7) and (8) is

$$y(k) = C(qI - A)^{-1} B u(k) + C(qI - A)^{-1} K e(k) + e(k) \tag{55}$$

which, in turn, is an auto regressive moving average with eXogenous inputs (ARMAX) parametric model defined as

$$\bar{A}(q^{-1}) y(k) = \bar{B}(q^{-1}) u(k) + \bar{C}(q^{-1}) e(k) \tag{56}$$

with

$$\bar{A}(q^{-1}) = 1 + a_1 q^{-1} + \cdots + a_{n_x} q^{-n_x} \tag{57}$$

$$\bar{B}(q^{-1}) = b_1 q^{-1} + \cdots + b_{n_x} q^{-n_x} \in \mathbb{R}^{1\times n_u} \tag{58}$$

$$\begin{aligned} \bar{C}(q^{-1}) &= 1 + (k_1 + a_1) q^{-1} + \cdots + (k_{n_x} + a_{n_x}) q^{-n_x} \\ &= 1 + \alpha_1 q^{-1} + \cdots + \alpha_{n_x} q^{-n_x} \end{aligned} \tag{59}$$

where k_i is the $(n_x - i + 1)$th entry of K. The one-step prediction is given as [27]

$$\hat{y}(k, \theta_{\text{ARMAX}}) = \frac{\bar{C}(q^{-1}) - \bar{A}(q^{-1})}{\bar{C}(q^{-1})} y(k) + \frac{\bar{B}(q^{-1})}{\bar{C}(q^{-1})} u(k) \tag{60}$$

with

$$\theta_{\text{ARMAX}} = \begin{bmatrix} a_1 & \cdots & a_{n_x} & b_1 & \cdots & b_{n_x} & \alpha_1 & \cdots & \alpha_{n_x} \end{bmatrix}^T.$$

From (28), (34), and (57)–(59)

$$\frac{\bar{C}(q^{-1}) - \bar{A}(q^{-1})}{\bar{C}(q^{-1})} = C(qI - A_0)^{-1} K \tag{61}$$

and

$$\begin{aligned} \frac{\bar{B}(q^{-1})}{\bar{C}(q^{-1})} &= C(qI - A_0)^{-1} B u(k) \\ &= \sum_{i=1}^{n_u} C(qI - A_0)^{-1} B_i u_i(k). \end{aligned} \tag{62}$$

If in (14), (15), and (18) L is replaced by its optimal value, K, then $e_y(k)$ becomes the PEM

$$\hat{e}(k, \theta_{\text{ARMAX}}) = y(k) - \hat{y}(k) = e(k). \tag{63}$$

Thus, minimizing the cost function (33) is equivalent to minimize the ARMAX PEM quadratic criterion

$$J_{\text{ARMAX}}(\theta) = \frac{1}{2} \sum_{k=1}^{N} \hat{e}(k, \theta_{\text{ARMAX}}) \tag{64}$$

performed by the *armax* command of the system identification toolbox of MATLAB. The advantage of the MOLI-PEM estimator is the reduced dimension of the optimization space which leads to more efficient algorithms.

IV. Model Estimation and Validation

In this section, the model estimation and validation strategy used to identify black-box models of a selected *Just Walk* participant with data according to Fig. 5 is discussed, and the results from fitting state-space models with the MOLI algorithms are presented and compared with standard ARX predictions. From what it was noted previously, by setting the estimate of K to L, the MOLI algorithms estimate the state-space innovation models form depicted in (7) and (8) and these are equivalent to ARMAX models defined in (56), where $y(k)$ is the measured output (e.g., steps/day), $u_i(k)$ is the measured input i, $e(k)$ is the PEM, all measured/estimated at day k, with k_i being the $(n_x - i + 1)$th entry of K. The orders of the polynomials $\bar{A}(q^{-1})$ and $\bar{B}_i(q^{-1})$ do not have to be the same. If the orders of $\bar{A}(q^{-1})$ and $\bar{B}_i(q^{-1})$, $i = 1, \ldots, n_u$ are n_a and n_{b_i}, the order of the state-space model is $n = \max(n_a, n_{b_1}, \ldots, n_{b_{n_u}})$ and

$$\ell_j = \alpha_j, \quad j > n_a$$
$$b_{i_j} = 0, \quad j > n_{b_i}$$

where ℓ_j is the $(n_x + j - 1)$th entry of L. These restrictions were introduced in the MOLI algorithms so they can estimate state-space realizations of MISO ARMAX models with different polynomial orders.

Preprocessed data were fit to innovation models in the observable canonical form equivalent to the ARMAX model structure ARMAX-$[n_a, n_{b_1}, \ldots, n_{b_{n_u}}, n]$ of (56). The innovation models were estimated by the ARX, Barycentre (polytope and random versions), Output and Separable Least Squares (PEM) versions of the MOLI algorithm. In data preprocessing, missing points were linearly interpolated, all input and output measurements were mean subtracted, and forward shifted as it was necessary to establish temporal precedence (i.e., causality/strict properness). To evaluate the goodness of fit, the index of FIT (IFIT) is defined as

$$\text{IFIT} = \left(1 - \sqrt{\frac{\sum_{k\in\mathcal{D}} \|y(k) - y_s(k)\|_2^2}{\sum_{k\in\mathcal{D}} \|y(k) - \bar{y}\|_2^2}}\right)100\% \qquad (65)$$

where

$$\bar{y} = \frac{1}{N_{\mathcal{D}}} \sum_{k\in\mathcal{D}} y(k)$$

with $N_{\mathcal{D}}$ being the total number of points in $\mathcal{D}$, was used. The model structure selection was achieved exhaustively by examining a range of model orders, then using model validation to determine the most predictive, parsimonious structure. In this case study, ARMAX model order ranges for n_a and n_{b_i} from 1 to 3 (i.e., $\max(n_a) = 3$, and $\max(n_{b_i}) = 3$ for $i = 1, \ldots, n_u$) while $n_c = n_x$, the order of $\bar{C}(q^{-1})$, equal to $n_x = \max(n_a, n_{b_1}, \ldots, n_{b_{n_u}})$ seemed reasonable. It should be noted that from the SCT fluid model (Fig. 1) and results presented in [14], it was known, *a priori*, that higher order models would not be necessary.

Given the multisine input signal design presented in Section II-A, at an individual level, the full data set was segmented into five 16-day cycles either for model estimation or validation (Fig. 5). Cross-validation represents one of the most valuable aspects of system identification [28]. The conventional approach is to assign a certain percentage of data for estimation, followed by validation (e.g., 50% estimation and 50% validation); such an approach assumes that the noise characteristics of the problem remain unchanged during the course of the intervention. However, it is reasonable to expect that noise and disturbance dynamics will vary over long-duration interventions such as *Just Walk*.

In the analysis, all combinations of data cycles involving at least two cycles for the validation were generated and evaluated (see first two columns in Table I). To handle this, the ARX, Barycentre (polytope and random versions), Output and Separable Least Squares (PEM) versions of the MOLI algorithms had to be adapted to estimate models from discontinuous data segments. This was achieved by considering each segment as a data stream with a regressor consisting of the observability matrix and the filtered signals $y_f(k)$ and $u_f(k)$ defined by (16) and (17) of this particular segment. All the regressors were fused in a single one to estimate the system parameters together with the initial states of each segment.

The output MOLI algorithm was initialized with the ARX estimates while the separable least squares were initialized with the ARX (PEMARX), and both the polytopic (PEMPoly) and random (PEMRandom) versions of the Barycentre MOLIZoft. For each combination of estimation segments and each algorithm, the models with the best IFIT index over the validation data were picked. However, it was observed that there were several models with good average IFIT index over the validation data but with a meaningless overall fit index. This was mainly due to the instability of the estimated models and the short length of the data segments that prevented the unstable modes to *explode*. The overall fit revealed to be much more reliable and, together with the average validation, was adopted to select the best model. Hence, the best-estimated model by each algorithm was the one with the best overall fit among the ones with the best average validation indexes.

Table I summarizes results of the PEMPoly algorithm using the above-mentioned strategy for a three-input model (*Goals*, *Expected Points*, and *Granted Points*) of a selected participant. Columns 3–10 show the calculated fit index from (65) over the estimation, validation, and the full (overall) data set. All evaluated cycle combinations feature at least two cycles for validation or estimation (twenty candidate models). For each of these combinations of estimation and validation cycles (corresponding to a specific row in Table I), the polynomial orders were determined from an exhaustive search routine that selects the model with highest predictive ability (based on the maximum average validation fit); this step provides a safeguard against overparametrization. The final chosen model should reflect, in addition to a good fit to validation data, a good fit over the entire data set (consisting of both estimation and validation cycles). This suggests that the final model choice should correspond to the model that yields highest overall fit (the "Overall IFIT Fit" column in Table I). Incorporating the overall fit criterion with the fit to cross-validation data balances good prediction with model accuracy over the entire data set.

TABLE I

INTERMEDIATE RESULTS FOR A THREE-INPUT MODEL OF A SELECTED PARTICIPANT FROM *Just Walk* ESTIMATED WITH THE PEM-MOLI ALGORITHM INITIALIZED WITH POLYTOPE-MOLIZOFT

E*	V*	IFIT (%)					Av. Est. IFIT (%)	Av. Val. IFIT(%)	Overall IFIT (%)	orders n_a, n_{b_1},n_{b_2}, n_{b_3}
		Cycle 1	Cycle 2	Cycle 3	Cycle 4	Cycle 5				
1,2	3,4,5	78.02	85.85	70.23	32.22	16.33	81.33	33.93	41.66	2,2,2,1
1,3	2,4,5	73.60	87.32	80.02	25.59	11.12	77.12	26.03	38.09	1,1,1,3
1,4	2,3,5	78.64	75.49	65.25	76.74	58.58	77.92	64.34	$-\infty$	1,2,2,3
1,5	2,3,4	71.94	79.58	68.23	58.08	44.16	52.36	67.65	52.07	3,3,2,1
2,3	1,4,5	74.83	73.47	81.58	26.31	7.01	78.19	24.51	30.37	2,3,1,2
2,4	1,3,5	72.97	78.03	60.32	70.52	52.44	73.89	59.67	$-\infty$	1,3,2,3
2,5	1,3,4	64.65	67.49	65.14	60.65	45.89	51.81	64.12	$-\infty$	2,3,3,2
3,4	1,2,5	69.42	69.13	70.18	56.41	38.06	64.42	51.31	$-\infty$	3,3,2,2
3,5	1,2,4	71.40	78.08	70.66	56.97	44.86	54.64	67.54	$-\infty$	2,3,2,1
4,5	1,2,3	63.52	57.64	60.09	54.88	46.84	49.40	60.62	42.70	2,3,2,1
1,2,3	4,5	76.31	81.26	77.47	28.62	11.42	78.17	16.80	36.04	2,2,1,2
1,2,4	3,5	74.76	80.85	64.63	53.82	37.74	67.57	48.20	53.19	1,3,2,1
1,2,5	3,4	68.37	72.54	67.28	59.75	45.17	56.11	64.59	54.37	3,3,3,2
1,3,4	2,5	70.80	83.48	72.21	31.86	13.90	56.60	28.23	39.75	2,3,1,1
1,3,5	2,4	70.75	76.16	66.93	48.00	35.43	51.55	58.96	47.23	1,3,2,1
1,4,5	2,3	64.48	57.24	61.56	29.06	15.78	29.31	60.11	34.39	1,1,3,2
2,3,4	1,5	78.21	84.18	69.58	40.47	22.07	61.28	36.15	46.19	3,2,2,1
2,3,5	1,4	73.41	71.84	65.29	42.81	20.65	41.83	55.99	41.34	1,2,1,2
2,4,5	1,3	65.96	66.69	62.92	39.32	26.20	37.03	64.23	37.02	3,3,1,1
3,4,5	1,2	69.55	65.12	62.37	61.40	39.91	51.53	67.48	53.74	2,2,2,2

*E≡ Estimation Cycles (magenta) V≡ Validation Cycles (cyan)

TABLE II

BEST THREE-INPUT MODELS FOR THE SELECTED PARTICIPANT DATA FROM *Just Walk*

alg	Est Seg	Model order	Av Val (%)	Overall fit (%)	Step Response @ $t = 1$
arx	2 3 5	3 3 1 1	52.19	41.71	0.84
polytope	1 2 4	1 3 2 2	45.20	51.84	0.80
random	2 4 5	3 3 2 1	64.90	51.25	0.69
outMoli	2 4	2 2 2 3	58.54	54.45	0.68
pemPoly	1 2 5	3 3 3 2	64.59	54.37	0.83
pemARX	2 3 5	3 2 2 1	57.04	47.71	0.88
pemRand	1 2 5	2 3 3 2	64.89	53.06	0.82

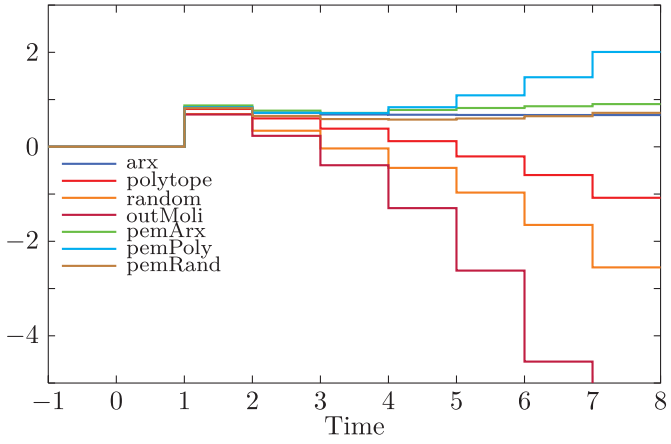

Fig. 6. Step responses of the best models for the transfer function from goals to actual steps, for the participant data according to Fig. 5.

Using this analysis, the best results for the selected participant and estimation algorithm occur in the model resulting from row 13 (cycles 1, 2, and 5 for estimation; 3 and 4 for validation; highlighted in yellow) with an overall IFIT index of 54.37% for a model with structure $n_a = 3$, $n_{b_1} = 3$, $n_{b_2} = 3$, and $n_{b_3} = 2$. This model performs close to the model with best fit over the validation data (average validation fit of 64.59% for row 13 versus 67.65% in row 4); however, the model with the best fit to validation data does not yield the best fit to data overall (52.07% in lieu of 54.37%). Because of instability, some models exhibit a meaningless overall fit (denoted as $-\infty$ in Table I) despite of having a good validation fit.

As expected the ARXMOLI models were equal to the models estimated by the `arx` command of the MATLAB System Identification Toolbox. Generally, these models displayed poorer fits than the ones estimated by the other versions of the MOLIZoft. Table II shows the best three-input models of the participant for each identification algorithm. All models show similar initial step responses (Fig. 6), with the magnitude at $t = 1$ (Table II) ranging from 0.68 to 0.88 steps per unit goal (average 0.79, std. dev. 0.07), indicating that this participant was highly responsive and compliant to the intervention. The best models in Table II are almost all unstable.

The Bode plots, depicted in Fig. 7, show that all models had similar frequency responses for the range of frequencies of the input signals, i.e., for frequencies greater than 0.4, the lowest frequencies of the input signal (see Fig. 7). Hence, identified models can only reproduce the high-frequency behavior and are inaccurate at low frequencies, exhibiting inconsistent step responses. This is illustrated in Fig. 8 that shows the step responses filtered by a high-pass fourth-order Butterworth filter with cutoff frequency of 0.4. From these results, it can be concluded that to estimate models with more uniform step responses, the *Just Walk* experiment should be redesigned with an input signal displaying power at lower frequencies.

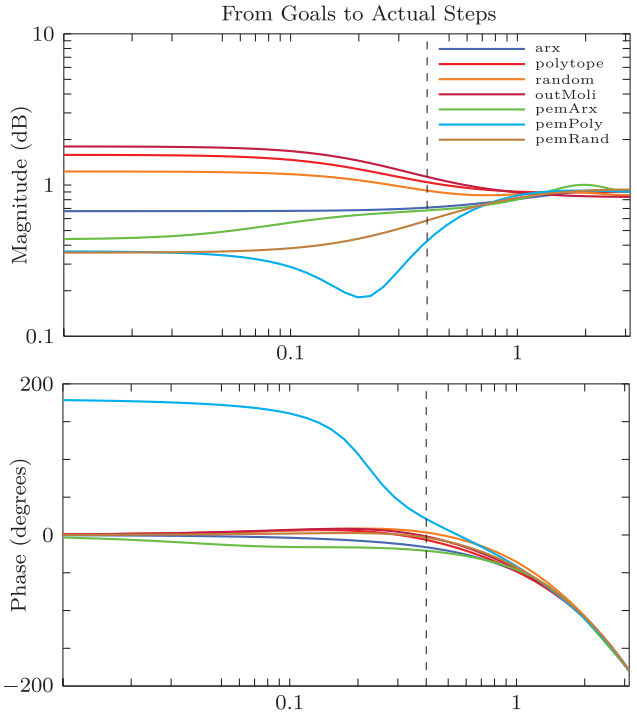

Fig. 7. Bode plots of the best models for the transfer function from goals to actual steps for the participant data according to Fig. 5.

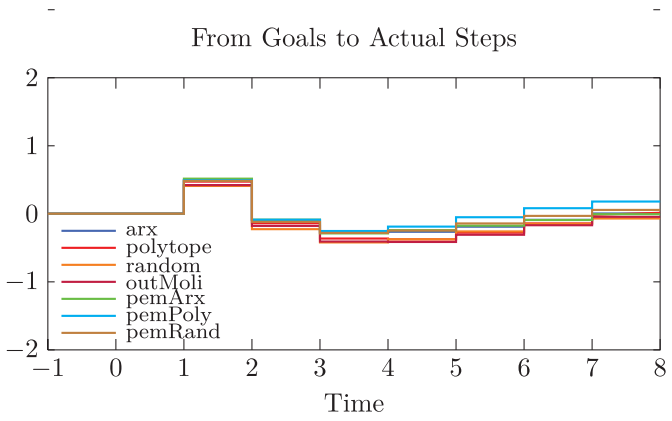

Fig. 8. Filtered step responses of the best models for the transfer function from goals to actual steps for the participant data according to Fig. 5.

V. Conclusion

In this paper, system identification of the *Just Walk* PA intervention has been presented. An input signal design and experimental execution procedure using multisines with "zippered" spectra were described. Next, a class of algorithms, denoted as MOLIZoft, was reformulated and adapted to estimate LTI models from the data gathered in an experiment for a selected intervention participant. By exploiting different possibilities to choose design variables, the following versions of the MOLIZoft algorithms were developed.

1) Least squares ARX (equivalent to the MATLAB's system identification toolbox `arx` command).
2) Polytopic barycentre optimization.
3) Random barycentre optimization.
4) Output error optimization.
5) Prediction error optimization with a separable least squares algorithm.

These algorithms were adapted to estimate state-space realizations of input–output models with polynomial orders ranging from 1 to 3 from discontinuous data sets. They were tested with participant data and produced more accurate models than the MATLAB's system identification toolbox command `arx`. While the initial step responses were similar, some models were unstable with significant differences in the step response at the final time. The analysis revealed that the frequency responses were similar in the range of frequencies with the power in the input signal; consequently, the inconsistency in the step responses was attributed to a lack of low-frequency excitation. Future work calls for a redesign of the *Just Walk* study with input signals that will include additional low-frequency harmonics. A consequence of such redesign is a longer cycle length; however, an incidental benefit of a longer cycle is that the signals will appear more pseudorandom to participants; this is an important consideration in designing acceptable trials in behavioral interventions.

Further, indications from the *Just Walk* data suggest the existence of time-varying dynamics on an individual level; consequently, alternative approaches, such as linear parameter varying system identification, should also be considered to estimate additional sets of black-box models that characterize dynamics that vary over time. The ultimate goal of the MOLI black-box models is to guide the development of personalized semiphysical (gray box) models conforming to the SCT structure in Fig. 1. Questions relating to which inputs have the greatest influence, how the semiphysical parameter estimation problem (potentially highly nonconvex) will be initialized, and how output measurements must be weighted in the estimation problem are all questions that can be answered relying on existing and future black-box modeling results.

The ultimate use of both the black-box and semiphysical dynamical models is as internal models for hybrid model predictive controllers acting as decision policies in an intervention; this is described in [1] and [13].

Acknowledgment

The opinions expressed in this paper are the authors' own and do not necessarily reflect the views of Fundação para a Ciência e a Tecnologia, SYSTEC, or National Science Foundation.

References

[1] D. E. Rivera, C. A. Martín, K. P. Timms, S. Deshpande, N. N. Nandola, and E. Hekler, "Control systems engineering for optimizing behavioral mhealth interventions," in *Mobile Health: Sensors, Analytic Methods, and Applications*, J. M. Rehg, S. A. Murphy, and S. Kumar, Eds. Cham, Switzerland: Springer, 2017, pp. 455–493.

[2] K. Bekiroglu, C. Lagoa, S. A. Murphy, and S. T. Lanza, "Control engineering methods for the design of robust behavioral treatments," *IEEE Trans. Control Syst. Technol.*, vol. 25, no. 3, pp. 979–990, May 2017.

[3] J. Ni, D. Kulić, and D. E. Davison, "A model-based feedback-control approach to behavior modification through reward-induced attitude change," in *Proc. Amer. Control Conf. (ACC)*, Jun. 2013, pp. 1956–1963.

[4] U. E. Bauer, P. A. Briss, R. A. Goodman, and B. A. Bowman, "Prevention of chronic disease in the 21st century: Elimination of the leading preventable causes of premature death and disability in the USA," *Lancet*, vol. 384, no. 9937, pp. 45–52, 2014.
[5] N. Owen, A. Bauman, and W. Brown, "Too much sitting: A novel and important predictor of chronic disease risk?" *Brit. J. Sports Med.*, vol. 43, no. 2, pp. 81–83, Dec. 2009.
[6] W. L. Haskell, S. N. Blair, and J. O. Hill, "Physical activity: Health outcomes and importance for public health policy," *Preventive Med.*, vol. 49, no. 4, pp. 280–282, 2009.
[7] L. M. Collins, S. A. Murphy, and K. L. Bierman, "A conceptual framework for adaptive preventive interventions," *Prevention Sci.*, vol. 5, no. 3, pp. 185–196, Sep. 2004.
[8] D. E. Rivera, M. D. Pew, and L. M. Collins, "Using engineering control principles to inform the design of adaptive interventions: A conceptual introduction," *Drug Alcohol Dependence*, vol. 88, no. 2, pp. S31–S40, 2007.
[9] W. Nilsen *et al.*, "Modeling opportunities in mhealth cyber-physical systems," in *Mobile Health: Sensors, Analytic Methods, and Applications*, J. M. Rehg, S. A. Murphy, and S. Kumar, Eds. Cham, Switzerland: Springer, 2017, pp. 443–453.
[10] A. Bandura, "Human agency in social cognitive theory," *Amer. Psychol.*, vol. 44, no. 9, pp. 1175–1184, 1989.
[11] C. A. Martín *et al.*, "A dynamical systems model of social cognitive theory," in *Proc. Amer. Control Conf. (ACC)*, Jun. 2014, pp. 2407–2412.
[12] C. A. Martín *et al.*, "Development of a control-oriented model of social cognitive theory for optimized mHealth behavioral interventions," *IEEE Trans. Control Syst. Technol.*, to be published, doi: 10.1109/TCST.2018.2873538.
[13] C. A. Martín, D. E. Rivera, and E. B. Hekler, "A decision framework for an adaptive behavioral intervention for physical activity using hybrid model predictive control," in *Proc. Amer. Control Conf. (ACC)*, Jul. 2016, pp. 3576–3581.
[14] M. T. Freigoun *et al.*, "System identification of just walk: A behavioral mHealth intervention for promoting physical activity," in *Proc. Amer. Control Conf. (ACC)*, May 2017, pp. 116–121.
[15] R. A. Romano and F. Pait, "Linear multivariable identification using observable state space parameterizations," in *Proc. 52nd IEEE Conf. Decis. Control*, Dec. 2013, pp. 1429–1434.
[16] R. A. Romano and F. Pait, "Direct filter tuning and optimization in multivariable identification," in *Proc. 53rd IEEE Conf. Decis. Control*, Dec. 2014, pp. 1798–1803.
[17] R. A. Romano and F. Pait, "Matchable-observable linear models and direct filter tuning: An approach to multivariable identification," *IEEE Trans. Autom. Control*, vol. 62, no. 5, pp. 2180–2193, May 2017.
[18] R. A. Romano, F. Pait, and R. C. Ferrão, "Matchable-observable linear models for multivariable identification: Structure selection and experimental results," in *Proc. 54th IEEE Conf. Decis. Control*, Dec. 2015, pp. 3391–3396.
[19] P. Lopes dos Santos *et al.*, "A MoliZoft system identification approach of the just walk data," *IFAC-PapersOnLine*, vol. 50, no. 1, pp. 12508–12513, 2017.
[20] T. Bohlin, *Practical Grey-box Process Identification: Theory and Applications* (Advances in Industrial Control). London, U.K.: Springer, 2006.
[21] S. Shiffman, A. A. Stone, and M. R. Hufford, "Ecological momentary assessment," *Annu. Rev. Clin. Psychol.*, vol. 4, no. 1, pp. 1–32, 2008.
[22] E. V. Korinek *et al.*, "Adaptive step goals and rewards: A longitudinal growth model of daily steps for a smartphone-based walking intervention," *J. Behav. Med.*, vol. 41, no. 1, pp. 74–86, Feb. 2018.
[23] D. E. Rivera, H. Lee, H. D. Mittelmann, and M. W. Braun, "Constrained multisine input signals for plant-friendly identification of chemical process systems," *J. Process Control*, vol. 19, no. 4, pp. 623–635, 2009.
[24] P. Guillaume, J. Schoukens, R. Pintelon, and I. Kollar, "Crest-factor minimization using nonlinear Chebyshev approximation methods," *IEEE Trans. Instrum. Meas.*, vol. 40, no. 6, pp. 982–989, Dec. 1991.
[25] S. S. Phatak *et al.*, "Modeling individual differences: A case study of the application of system identification for personalizing a physical activity intervention," *J. Biomed. Inform.*, vol. 79, pp. 82–97, Mar. 2018.
[26] L. Kaufman, "A variable projection method for solving separable nonlinear least squares problems," *BIT Numer. Math.*, vol. 15, no. 1, pp. 49–57, 1975.
[27] L. Ljung, *System Identification: Theory for the User*. Upper Saddle River, NJ, USA: Prentice-Hall, 1987.
[28] L. Ljung, "From data to model: A guided tour," in *Proc. Int. Conf. Control (Control)*, vol. 1, Mar. 1994, pp. 422–430.

Paulo Lopes dos Santos (M'08) was born in Porto, Portugal, in 1958. He received the Licenciatura degree in electrical engineering, the M.Sc. degree in computers and digital systems, the Ph.D. degree in electrical engineering, and the Agregado degree from Oporto University, in 1981, 1987, 1994, and 2016, respectively.

From 1983 to 1994, he was an Assistant Lecturer with the Electrical Engineering Department, Oporto University, where he is currently a Lecturer in electrical engineering. From 1985 to 2018, he developed his research with the Institute for Systems and Robotics-Oporto, Porto. He is currently with the Institute for Systems and Computer Engineering, Technology and Science (INESC-TEC). His current research interests include system identification.

Dr. Lopes dos Santos is a member of the Control System Society, International Federation of Automatic Control, and Associação Portuguesa de Controlo Automático.

Mohammad T. Freigoun received the B.S. degree in chemical engineering from the University of Khartoum, Khartoum, Sudan, in 2010. He is currently pursuing the Ph.D. degree in chemical engineering with Arizona State University, Tempe, AZ, USA.

He was a Planning Engineer with the Supply Chain Management Department, Tabuk Pharmaceuticals Manufacturing Company, Khartoum, until 2013. His current research interests include mathematical modeling, system identification, and predictive control, including applications in biosystems and the design of optimized and perpetually adaptive interventions in behavioral health and medicine, developing and applying methods of systems engineering, and optimization in process systems and supply chain management problems.

César A. Martín (M'15) was born in Guayaquil, Ecuador, in 1971. He received the B.S. degree in electrical engineering and the M.B.A degree from Escuela Superior Politécnica del Litoral (ESPOL) Polytechnic University, Guayaquil, in 1993 and 1996, respectively, and the M.S.E. and Ph.D. degrees in electrical engineering from Arizona State University, Tempe, AZ, USA, in 2003 and 2016, respectively.

From 2012 to 2016, he was with the Control Systems Engineering Laboratory, Arizona State University. Since 1996, he has been an Associate Professor with the Department of Electrical and Computing Engineering, ESPOL Polytechnic University, where he is currently an Associate Dean. His current research interests include system identification, dynamic modeling, and control applications in behavioral medicine and agricultural settings.

Daniel E. Rivera (M'91–SM'05) received the B.S. degree in chemical engineering from the University of Rochester, Rochester, NY, USA, in 1982, the M.S. degree in chemical engineering from the University of Wisconsin–Madison, Madison, WI, USA, in 1984, and the Ph.D. degree in chemical engineering from the California Institute of Technology, Pasadena, CA, USA, in 1987.

He was a member of the Control Systems Section, Shell Development Company, Houston, TX, USA. He is currently a Professor of chemical engineering with the School for Engineering of Matter, Transport, and Energy, Arizona State University, Tempe, AZ, USA. His current research interests include system identification, robust process control, and applications of control engineering to problems in supply chain management and behavioral medicine.

Dr. Rivera has been the Chair of the IEEE Control System Society's (CSS's) Outreach Task Force since 2014. He was the Inaugural Chair of the IEEE CSS Technical Committee on Healthcare and Medical Systems from 2013 to 2014 and the Chair of the IEEE CSS Technical Committee on System Identification and Adaptive Control from 2007 to 2012. He was a recipient of the K25 Mentored Quantitative Research Career Development Award from the National Institutes of Health to study the application of control systems engineering principles to optimize personalized prevention and treatment interventions for drug abuse. He is a Past Associate Editor for the IEEE TRANSACTIONS IN CONTROL SYSTEMS TECHNOLOGY from 2003 to 2010 and *IEEE Control Systems Magazine* from 2003 to 2007.

Eric B. Hekler received the Ph.D. degree in clinical health psychology from Rutgers University, New Brunswick, NJ, USA.

He was a Post-Doctoral Trainee with Stanford University, Stanford, CA, USA. He was a Professor with Arizona State University, Phoenix, AZ, USA. He is currently an Associate Professor with the Department of Family Medicine and Public Health, University of California at San Diego (UCSD), San Diego, CA, USA, the Director of the Center for Wireless and Population Health Systems,Qualcomm Institute, UCSD, and a Faculty Member with the Design Laboratory, UCSD. He is involved in advancing methods via melding approaches from behavioral science/psychology, public health, human–computer interactions, control systems engineering, and computer science. There are three interdependent themes to his research for advancing: 1) methods for optimizing adaptive behavioral interventions; 2) methods and processes to help people help themselves; and 3) research pipelines to achieve efficient, rigorous, context-relevant solutions for complex problems. His current research interests include advancing methods in the design, creation, optimization, evaluation, and reuse (scaling up and out) of digital health technologies.

Rodrigo Alvite Romano (M'13) received the B.S. degree in electrical engineering from the Faculdade de Engenharia Industrial, São Bernardo do Campo, Brazil, and the M.Sc. and D.Sc. degrees in electrical engineering from the Escola Politécnica da Universidade de São Paulo, São Paulo, Brazil, in 2006 and 2010, respectively.

He is currently an Associate Professor with the Instituto Mauá de Tecnologia, São Caetano do Sul, Brazil. His current research interests include data-driven modeling and control of dynamic systems.

Teresa P. Azevedo Perdicoúlis was born in São João da Pesqueira, Portugal, in 1966. She received the Licenciatura degree in mathematics and computer Science from the University of Coimbra, Coimbra, Portugal, in 1991, the M.Sc. degree in electronic control engineering and the Ph.D. degree in mathematics and computational sciences from the University of Salford, Greater Manchester, U.K., in 1995 and 2000, respectively, under the supervision of L. R. Fletcher.

She was a Technical Representative with ICL, Coimbra, Portugal. She held a postdoctoral position in the field of differential games with the University of Aachen, Aachen, Germany, under the supervision of Prof. G. Jank. Since 1991, she has been with the University of Trás-os-Montes e Alto Douro (UTAD), Vila Real, Portugal, where she has occupied different positions. Since 1992, she has been a Researcher with ISR, University of Coimbra, Coimbra, Portugal, and an Invited Member of Systec, University of Porto, Porto, Portugal. Since 2009, she has been involved in system identification under the supervision of Dr. P. Lopes dos Santos. She is currently an Associate Professor with Tenure with UTAD. She has been teaching and responsible for various courses in mathematics and control systems engineering. She has co-authored more than 80 peer-reviewed scientific works and close to a dozen lecture notes in different subjects. Her current research interests include modeling optimization and simulation of gas networks.

Dr. Azevedo Perdicoúlis lis is a member of IFAC and APCA.